Heat shock protein 20 suppresses breast carcinogenesis by inhibiting the MAPK and AKT signaling pathways

YINXI YANG[1*], YIFENG WU[1*], LIHONG HOU[2], XIN GE[3], GUOQUAN SONG[1] and HONGDOU JIN[1]

[1]Department of General Surgery, Wuxi 9th People's Hospital Affiliated to Soochow University, Wuxi, Jiangsu 214000; [2]Department of Pathology, Jinzhou Maternal and Infant Hospital, Jinzhou, Liaoning 121000; [3]Department of ICU, Wuxi 9th People's Hospital Affiliated to Soochow University, Wuxi, Jiangsu 214000, P.R. China

Received May 6, 2022; Accepted October 10, 2022

DOI: 10.3892/ol.2022.13582

Abstract. Heat shock protein (HSP) 20 belongs to the small HSP family and exhibits diverse functions, including tumor suppression, in addition to being a molecular chaperon, which is the classical property of HSPs. The present study aimed to examine the association between HSP20 expression and breast cancer (BC) progression in patients, and to explore the possible role of HSP20 in malignant phenotypes of BC cells. A series of experiments, including reverse transcription-quantitative PCR, western blotting, Cell Counting Kit-8 and flow cytometry, were performed. Data from Gene Expression Omnibus and Kaplan-Meier Plotter revealed that HSP20 expression was significantly downregulated in BC tissues, and patients with BC with lower HSP20 expression exhibited poorer recurrence-free survival. The data revealed that HSP20 was closely associated with the pathological tumor stage (P=0.015) and pathological tumor node metastasis (P=0.031) of patients with BC. Additionally, HSP20 expression was markedly decreased in BC cell lines. Exogenous overexpression of HSP20 inhibited proliferation and accelerated apoptosis of BC cells. These cells exhibited decreased migration and invasion when HSP20 was overexpressed. Furthermore, HSP20 overexpression suppressed the MAPK and AKT signaling pathways, as evidenced by the reduced phosphorylation levels of AKT, ERK, JNK and p38. Knockdown of HSP20 exerted the opposite effects. Notably, the AKT agonist, SC79, and the ERK agonist, LM22B-10, reversed the decrease in cell proliferation and migration induced by HSP20 overexpression. Overall, the data suggest that the decreased expression of HSP20 in BC tissues may be associated with disease progression. HSP20 also attenuated the malignant phenotype of BC cells and the inhibition of MAPK and AKT signaling may be associated with this effect. Therefore, HSP20 may be a potential prognostic marker or a candidate therapeutic target for BC.

Correspondence to: Ms. Hongdou Jin, Department of General Surgery, Wuxi 9th People's Hospital Affiliated to Soochow University, 999 Liangxi Road, Binhu, Wuxi, Jiangsu 214000, P.R. China
E-mail: jinhongdou_scu@aliyun.com

*Contributed equally

Key words: heat shock protein 20, breast cancer, malignant phenotype, MAPK, AKT

Introduction

Breast cancer (BC), one of the most common tumor types, is the second leading cause of cancer-related mortality among females (1-3). In China, BC cases account for 12.2% of all new BC diagnoses worldwide and 9.6% of all BC-related deaths (4). In previous years, a number of treatments have been developed for improving the survival rate of patients with BC, including surgery, radiotherapy, chemotherapy, endocrine therapy and antibody therapy (5,6). The early diagnosis and treatment of the disease usually leads to a good prognosis with a high survival rate (7). However, patients diagnosed with advanced BC usually have a low survival rate and poor prognosis, and recurrence often occurs (8). The majority of deaths from BC are mainly due to drug resistance and metastasis to distant organs, such as the bone, liver, lungs and brain (9,10). Therefore, the development of novel biomarkers for the early diagnosis and treatment of BC is mandatory.

Recently, heat shock protein (HSP) 20 has become a hotspot for tumor research due to its role in regulating proliferation and apoptosis (11). As a molecular chaperone, HSP20 belongs to the small HSP family and is expressed in various organs (12). In 2007, HSP20 was found to be downregulated in hepatocellular carcinoma (HCC) tissues and was associated with tumor progression (13). Later, the detailed pathological mechanisms of HSP20 in HCC were reported by the same group (14-16). In addition, another research group reported decreased expression of HSP20 in colorectal cancer tissues (17). However, whether HSP20 serves a functional role in BC remains unclear.

MAPKs and AKT are responsible for intracellular signal transduction and are usually activated by phosphorylation in response to various stimuli (18,19). It is well known that MAPK-related factors, ERK, JNK and p38, serve a vital regulatory role in cell proliferation, invasion and metastasis (20-22). Notably, accumulating evidence suggests that

the inhibition of the MAPK and AKT signaling pathways can alleviate BC cell migration, invasion and proliferation (23,24). The present study aimed to explore whether HSP20 serves a regulatory role in BC through the MAPK and AKT signaling pathways.

In the present study, data from Gene Expression Omnibus (GEO) datasets and the Kaplan-Meier Plotter database were employed to investigate the expression of HSP20 in BC tissues and determine the association between HSP20 expression and the prognosis of patients with BC, respectively. The association of HSP20 with patient clinicopathological features was first identified and the effects of HSP20 on cell proliferation, migration and invasion were also examined. Mechanistically, the MAPK and AKT signaling pathways may be involved in the HSP20-mediated suppression of BC progression.

Materials and methods

Clinical samples. A total of 53 tumor samples were collected from female patients (age range, 33-82 years; mean age, 55 years) diagnosed with BC at Wuxi 9th Affiliated Hospital of Soochow University (Wuxi, China) between March 2021 and February 2022. The inclusion criteria were as follows: i) ≥18 years old; and ii) had never undergone any type of anticancer therapy, such as chemotherapy and radiotherapy prior to surgery. Patients diagnosed with other cancers were excluded. The use of human tissues was approved by the Ethics Committee of Wuxi 9th Affiliated Hospital of Soochow University (approval no. LW2021008; Wuxi, China), and written informed consent was provided by each participant. The expression of HSP20 was examined using immunohistochemical (IHC) staining of BC tissues, and the scoring system method was performed manually according to the literature (25). Briefly, the tumor samples were fixed in 4% paraformaldehyde for 24 h at room temperature and embedded in paraffin. The paraffin-embedded samples were cut into 5-μm thick sections. After dewaxing with xylene for 15 min, the sections were rehydrated with gradient alcohol solution (95, 85 and 75% for 2 min each) at room temperature. Following antigen retrieval by boiling in citrate buffer for 10 min in a microwave oven, H_2O_2 (3%) was added to the sections for 15 min. Subsequently, the sections were blocked with 1% goat serum (SL038; Beijing Solarbio Science & Technology Co., Ltd.) for 15 min at room temperature. Subsequently, the sections were incubated with anti-HSP20 (diluted 1:100; AF6003; Affinity Biosciences) at 4˚C overnight. The horseradish peroxidase-conjugated goat-anti-rabbit secondary antibody (diluted 1:500; #31460; Thermo Fisher Scientific, Inc.) was added for 1 h at 37˚C. The staining was visualized using 100 μl DAB chromogenic fluid (DA1010; Beijing Solarbio Science & Technology Co., Ltd.). Following hematoxylin counterstaining at room temperature for 3 min, sections were observed under a light microscope (magnification, x400; Olympus Corporation). The IHC scores of HSP20 expression are shown in Fig. S1A. The median value of HSP20 was a score of 2. If the HSP20 measurement was a score >2, it was considered high expression; if the HSP20 was a score ≤2, it was considered low expression. Representative IHC images are provided in Fig. S1B. The results of IHC scoring were used to divide patients into two groups [HSP20 high expression group (n=18) and HSP20 low expression group (n=35)]. Subsequently, the association between HSP20 and patient clinicopathological features was analyzed (Table I). Data from the GEO database [https://www.ncbi.nlm.nih.gov/geo/; GSE139038, n=18; GSE115144, n=21; GSE109169, n=25 (26,27)] were applied to evaluate the expression of HSP20 in paired BC tissues and adjacent non-cancerous tissues. The original data from GEO are shown in Table SI. The Kaplan-Meier Plotter database (http://kmplot.com/analysis/; survival curve, BC mRNA; gene symbol, 214767_s_at; split patients by median; follow up threshold, 120 months; cut-off value used in analysis, 172) was used to assess the association between HSP20 expression and the recurrence-free survival of 4,929 patients with BC.

Cells and cell culture. The MDA-MB-231, MDA-MB-453 and MDA-MB-468 human BC cell lines were incubated in L15 medium (LA9510; Beijing Solarbio Science & Technology Co., Ltd.) containing 10% FBS (SH30084.03; HyClone; Cytiva), 1% penicillin (C8251; Beijing Solarbio Science & Technology Co., Ltd.) and 1% streptomycin (S8290; Beijing Solarbio Science & Technology Co., Ltd.) in a 37˚C, 5% CO_2 incubator. The MCF-7 and ZR-75-1 cells were cultured with Minimum Essential Medium (MEM; 41500; Beijing Solarbio Science & Technology Co., Ltd.) containing 10% FBS, 1% penicillin (C8251; Beijing Solarbio Science & Technology Co., Ltd.) and 1% streptomycin (S8290; Beijing Solarbio Science & Technology Co., Ltd.) and RPMI-1640 (31800; Beijing Solarbio Science & Technology Co., Ltd.) medium containing 10% FBS, 1% penicillin (C8251; Beijing Solarbio Science & Technology Co., Ltd.) and 1% streptomycin (S8290; Beijing Solarbio Science & Technology Co., Ltd.) in a 37˚C, 5% CO_2 incubator, respectively. The MCF-10A cells were cultured in Mammary Epithelium Basal Medium (CC-3150; iCell Bioscience, Inc.) in a 37˚C, 5% CO_2 incubator. The MDA-MB-231, MDA-MB-453, MDA-MB-468, MCF-7 and MCF-10A cells were purchased from iCell Bioscience, Inc. The ZR-75-1 cells were purchased from Procell Life Science & Technology Co., Ltd.

Cell transfection. The plasmid containing pcDNA3.1-HSP20 (exHSP20) and HSP20 small interference RNA sequences (si-HSP20-1/2) were synthesized by GenScript and JTSBio, respectively. The corresponding vector or non-targeting control (si-NC) served as a negative control. The control group consisted of untransfected cells, and the vector group consisted of cells transfected with an empty vector. The sequences of si-HSP20-1/2 and si-NC were as follows: si-HSP20-1 sense, 5'-CGGUGCUGCUAGACGUGAATT-3' and antisense, 5'-UUCACGUCUAGCAGCACCGTT-3'; si-HSP20-2 sense, 5'-CGGAGGAAAUUGCUGUCAATT-3' and antisense, 5'-UUGACAGCAAUUUCCUCCGTT-3'; and si-NC sense, 5'-UUCUCCGAACGUGUCACGUTT-3' and antisense, 5'-ACGUGACACGUUCGGAGAATT-3'. The MDA-MB-231 and MDA-MB-468

Table I. Association between clinicopathologic parameters and HSP20 expression in 53 patients with breast cancer.

Clinical parameters	HSP20 expression		P-value
	High, n (n=18)	Low, n (n=35)	
Age, years			0.504
<50	3	10	
≥50	15	25	
ER			0.144
Positive	17	27	
Negative	1	8	
PR			0.539
Positive	14	24	
Negative	4	11	
HER2			0.174
Positive	10	11	
Negative	8	23	
Unknown	0	1	
Ki-67, %			0.901
<14	7	13	
≥14	11	22	
pT			0.015[a]
T1	6	20	
T2	5	10	
T3	0	3	
Tis	7	2	
pN			0.179
N0	13	23	
N1	3	5	
N2	2	1	
N3	0	6	
pStage			0.031[a]
0	7	2	
I	6	15	
II	3	10	
III	2	8	

[a]P<0.05. HSP20, heat shock protein 20; ER, estrogen receptor; PR, progesterone receptor; HER2, human epidermal growth factor receptor 2; pT, pathological tumor stage; pN, pathological lymph node metastasis; pStage, pathological tumor node metastasis.

cells were transfected with 2.5 μg exHSP20 plasmid or vector using Lipofectamine 3000® (Invitrogen; Thermo Fisher Scientific, Inc.) at 37˚C for 24 h. G418 (300 μg/ml; 11811023; Invitrogen; Thermo Fisher Scientific, Inc.) was then added to the cells for further selection, and stable HSP20-overexpressing cells were obtained in the presence of G418 (300 μg/ml) 2 weeks later. G418 (150 μg/ml) was added to stable HSP20-overexpressing cells for maintenance. The MCF-7 cells were transfected with 75 pmol si-HSP20-1/2 or si-NC at 37˚C for 48 h using Lipofectamine 3000® to obtain HSP20-silenced cells. Directly after transfection for 48 h, cells were harvested for the subsequent experiments.

RT-qPCR. Total RNA was extracted from the cells using TRIpure lysis buffer (BioTeke Corporation). The extracted RNA was treated with the BeyoRT II m-MLV reverse transcriptase kit (Beyotime Institute of Biotechnology) to obtain cDNA according to the manufacturer's instructions. The qPCR reaction system was then constructed according to the SYBR-Green (Beijing Solarbio Science & Technology Co., Ltd.) kit instructions. The thermocycling conditions were as follows: 94˚C for 5 min, followed by 40 cycles of 94˚C for 15 sec, 60˚C for 25 sec and 72˚C for 30 sec. Relative gene expression was calculated using the $2^{-\Delta\Delta Cq}$ method (28) and β-actin was used as an internal control. The details of primers used were as follows: HSP20 forward, 5'-CGGACGCCTCTTTGACCAG-3' and reverse, 5'-CGGTAGCGACGGTGGAACT-3'; and β-actin forward, 5'-CACTGTGCCCATCTACGAGG-3' and reverse, 5'-TAATGTCACGCACGATTTCC-3'.

Western blot analysis. Protein was extracted from the cells using IP cell lysate buffer (Beyotime Institute of Biotechnology) and the concentration was quantified using a BCA kit (Beyotime Institute of Biotechnology). Quantitative protein samples (~20 μg/lane) were separated on an 10% SDS-PAGE gel and transferred to PVDF (MilliporeSigma) membranes. The membranes were then blocked with 5% (w/v) skimmed milk at room temperature for 1 h. Subsequently, the membranes were incubated with the corresponding primary antibodies at 4˚C overnight. The membranes were then covered with HRP-conjugated goat-anti-rabbit/mouse secondary antibody (A0208 and A0216; diluted 1:5,000; Beyotime Institute of Biotechnology) at 37˚C for 45 min. After the bands were visualized using ECL (P0018; Beyotime Institute of Biotechnology), the optical density of each band was analyzed using Gel-Pro-Analyzer software (version 4.0; Beijing Liuyi Biotechnology Co., Ltd.). The primary antibodies used were as follows: Anti-HSP20 (AF6003; diluted 1:500), anti-phosphorylated (p-)ERK (AF1015; diluted 1:500), anti-ERK (AF0155; diluted 1:500), anti-p-JNK (AF3318; diluted 1:1,000), anti-JNK (AF6318; diluted 1:500), anti-p-AKT (#4060; diluted 1:1,000), anti-AKT (#4691; diluted 1:2,000), anti-Bax (A19684; diluted 1:500), anti-Bcl-2 (A0208; diluted 1:1,000), anti-caspase-3 (#14220; diluted 1:1,000), anti-poly (ADP-ribose) polymerase (PARP; #9542; diluted 1:1,000), anti-p-p38 (bs-0636R; diluted 1:400), anti-p38 (bs-0637R; diluted 1:500). HSP20, p-ERK, ERK, p-JNK and JNK antibodies were purchased from Affinity Biosciences. The p-AKT, AKT, caspase-3 and PARP antibodies were purchased from Cell Signaling Technology, Inc. The Bax and Bcl-2 antibodies were purchased from ABclonal Biotech Co., Ltd. The p-p38 and p38 antibodies were purchased from BIOSS. The internal reference β-actin antibody (sc-47778; diluted 1:1,000) was purchased from Santa Cruz Biotechnology, Inc.

Cell viability assay. The cells in each group were seeded in 96-well plates ($4x10^3$ cells/well) and incubated at 37˚C for 0, 24, 48 and 72 h, respectively. Following incubation, cell

viability was detected using a Cell Counting Kit-8 (CCK-8; MilliporeSigma). Briefly, the cells were covered with the CCK-8 reagent (10 μl/well) for 2 h. Subsequently, the optical density values were measured at 450 nm using a microplate reader.

In rescue experiments, HSP20-overexpressing stable MDA-MB-231 cells were treated with 10 μM SC79 (S80614; Yuanye Biology) or 50 μM LM22B-10 (L879472; Macklin, Inc.) at 37˚C for 48 h. Subsequently, a CCK-8 assay was performed as aforementioned.

Colony formation assay. The MDA-MB-231 and MDA-MB-468 cells ($3x10^2$ cells/plate) were plated into a 35-mm cell culture plastic and incubated at 37˚C with 5% CO_2 for ~2 weeks. Colonies were fixed in 4% paraformaldehyde at room temperature for 20 min and stained with Ray-Giemsa dye (Nanjing KeyGen Biotech Co., Ltd.) at room temperature for 5 min, then visualized and counted manually. Colonies consisted of >50 cells. The colony formation rate=colony number/300x100%.

Apoptosis detection. The apoptosis of the MDA-MB-231 and MDA-MB-468 cells was analyzed using an Annexin V-FITC Apoptosis Detection Kit (C1062; Beyotime Institute of Biotechnology). All reagents mentioned in this subsection were included in this kit. In brief, the cells were washed twice with PBS and mixed with 195 μl Annexin V-FITC binding buffer. The cells were then incubated with 5 μl Annexin V-FITC and 10 μl PI in the dark at room temperature for 15 min. Subsequently, a NovoCyte flow cytometer (ACEA Bioscience, Inc.) was used to evaluate cell apoptosis. The apoptotic cells were analyzed using NovoCyte software (version 1.5.6, ACEA Bioscience, Inc.).

Wound healing assay. After the MDA-MB-231, MDA-MB-468 and MCF-7 cells (reached 100% confluency) were incubated in serum-free medium supplemented with 1 μg/ml mitomycin C (MilliporeSigma) for 1 h, a 200-μl pipette tip was used to create a scratch. The cells treated with or without SC79 (10 μM)/LM22B-10 (50 μM) were cultured at 37˚C for 24 h. Cell fragments were removed by washing with PBS. Subsequently, cells were observed under a light microscope at x100 magnification and images were captured. The distance of the wound was measured using ipwin32 (version 6.0; National Institutes of Health). Migration rate=distance from edge at 24 h/distance from edge at 0 h x100%.

Cell invasion assay. For the cell invasion assay, 24-well Transwell chambers (Corning, Inc.) were applied. After the Matrigel was added to the upper chambers at 37˚C for 2 h, cells ($3x10^4$) were suspended in serum-free L15 medium or MEM (200 μl) and seeded on it. L15 medium or MEM supplemented with 10% FBS (800 μl) was added to the lower chamber. After incubation at 37˚C for 24 h, paraformaldehyde (4%) was used to fix the invasive cells. The cells were then stained with 0.4% crystal violet solution at room temperature for 5 min and observed under a light IX53 microscope at a magnification of x200 (Olympus Corporation).

Statistical analysis. The statistical analysis was carried out using GraphPad Prism (V8.0; GraphPad Software, Inc.). A paired Student's t-test was used for comparisons between two groups. One-way ANOVA with Tukey's post hoc test was used for multiple group comparisons. Pearson's χ^2 test (Ki-67) or Fisher's exact test (age, ER, PR, HER2, pT, pN and pStage) was performed to examine the association between the HSP20 expression and the patient clinicopathologic characteristics. Experiments were performed in triplicate. All experimental data are presented as the mean ± SD. $P<0.05$ was considered to indicate a statistically significant difference.

Results

Decreased HSP20 expression is associated with disease progression and prognosis of patients with BC. Data from three published GEO datasets (GSE139038, GSE115144 and GSE109169) revealed that HSP20 expression was downregulated in BC tissues compared with in paired non-cancer tissues (Fig. 1A). In addition, the results from the Kaplan-Meier Plotter database indicated that low HSP20 expression was significantly associated with the poor prognosis of patients with BC (Fig. 1B). Furthermore, the present study analyzed the association between HSP20 expression and the clinicopathological parameters of 53 patients diagnosed with BC. The clinicopathological characteristics are presented in Table I. The results illustrated that HSP20 expression was markedly associated with the pathological tumor stage [pT: T1, T2, T3 and Tis; according to the staging system of the International Union Against Cancer (29)] and pathological tumor node metastasis [pStage: N0, N1, N2 and N3; according to the staging system of the International Union Against Cancer (29)] of BC.

HSP20 inhibits BC cell proliferation. The results of RT-qPCR and western blot analysis revealed that HSP20 expression was significantly decreased in five BC cell lines compared with the MCF-10A normal mammary epithelial cell line (Fig. 2A). Among these cell lines, the two cell lines with the lowest expression of HSP20, MDA-MB-231 (relative protein expression of HSP20, 0.16) and MDA-MB-468 (relative protein expression of HSP20, 0.23), were selected to establish stable HSP20-overexpressing cell lines. Additionally, the MCF-7 cell line is hormone receptor-positive and is the most common subtype of BC. The MCF-7 cell line with relatively high HSP20 protein expression (0.53) was selected to establish the HSP20-silenced cell line. The analysis of the transfection efficiency demonstrated that the mRNA and protein expression levels of HSP20 in the exHSP20 group were significantly enhanced compared with those of the empty vector group (Fig. 2B). Additionally, HSP20 expression was successfully silenced in MCF-7 cells (Fig. S2A).

In order to investigate the association between HSP20 and cell proliferation, CCK-8 and colony formation assays were performed. The results revealed that overexpression of HSP20 markedly decreased cell viability (Fig. 2C), while knockdown of HSP20 exerted opposite effects (Fig. S2B). Consistently, the colony formation assay confirmed that the overexpression of HSP20 inhibited BC cell colony formation

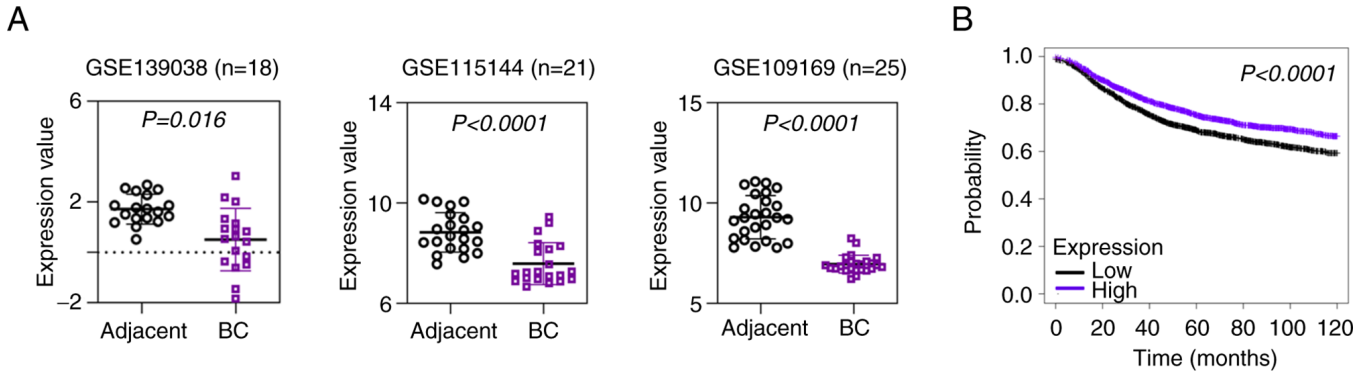

Figure 1. HSP20 expression in the tissues of patients with BC, and the association between HSP20 expression and recurrence-free survival. (A) Gene Expression Omnibus datasets were used to estimate HSP20 expression in BC tissues and adjacent non-cancer tissues (GSE139038, n=18; GSE115144, n=21; GSE109169, n=25). (B) Data from the Kaplan-Meier Plotter database showed that low HSP20 expression was associated with poor prognosis of patients with BC (n=4,929). BC, breast cancer; HSP20, heat shock protein 20.

(Fig. 2D). These data suggested that HSP20 suppressed BC cell proliferation.

HSP20 promotes BC cell apoptosis. To clarify the association between HSP20 and cell apoptosis, flow cytometric analysis was performed to evaluate cell apoptosis. The apoptotic rate of the exHSP20 group was observably enhanced compared with that of the empty vector group (Fig. 3A). In addition, the protein levels of pro-PARP, cleaved (active) PARP, pro-caspase-3, cleaved (active) caspase-3, Bcl2 and Bax were examined using western blot analysis. The results indicated that the levels of cleaved PARP/pro-PARP, cleaved caspase-3/pro-caspase-3 and Bax were significantly upregulated, whereas the level of Bcl-2 was significantly downregulated in HSP20-overexpressing BC cells (Fig. 3B). These findings indicated that overexpression of HSP20 facilitated BC cell apoptosis.

HSP20 suppresses BC cell migration and invasion. Subsequently, the present study verified the effects of HSP20 on BC cell migration and invasion. As shown in Fig. 4A, the results of the wound healing assay revealed that overexpression of HSP20 decreased migration, while knockdown of HSP20 increased the BC cell migration rate (Fig. S2C). In addition, the results of the Transwell assay demonstrated that the number of invaded cells in the exHSP20 group was significantly reduced (Fig. 4B). These results revealed that HSP20 inhibited the migration and invasion of BC cells.

HSP20 inhibits the AKT and MAPK signaling pathways. The AKT and MAPK signaling pathways are two crucial signaling pathways in cancer (22,23). In the present study, the results of western blot analysis indicated that HSP20 overexpression suppressed the AKT and MAPK signaling pathways, as evidenced by the reduced phosphorylation levels of AKT, as well as ERK, JNK and p38 in BC cells (Fig. 5A and B). However, HSP20 silencing exerted the opposite effects (Fig. S2D). Thus, the regulatory effects of HSP20 on the malignant phenotype of BC cells may be associated with the inhibition of these two signaling pathways.

SC79 or LM22B-10 treatment reverses the inhibitory effects of HSP20 on cell proliferation and migration. The AKT and ERK agonists, SC79 and LM22B-10, were applied in rescue experiments. MDA-MB-231 cells were randomly selected for these experiments. As demonstrated by the CCK-8 assay, the decreased cell viability induced by HSP20 overexpression was reversed by SC79 or LM22B-10 treatment (Fig. 6A). Consistently, SC79 or LM22B-10 treatment also reversed the suppressive effects of HSP20 overexpression on the migration of MDA-MB-231 cells (Fig. 6B).

Discussion

The mortality of patients with BC is usually ascribed to cell metastasis (30,31). HSP20 participates in a number of pathological processes, including the prevention of vasospasms, insulin resistance and cardioprotection (32,33). Furthermore, HSP20 has become a research hotspot in the field of cancer; however, the function of HSP20 in BC is not yet fully understood. The present study demonstrated that HSP20 expression was downregulated in BC tissues and BC cell lines, which was associated with clinicopathological pT and pStage parameters in patients with BC. It was further demonstrated that HSP20 suppressed cell proliferation, migration and invasion by inhibiting the MAPK and AKT signaling pathways.

One hallmark of cancer cells is the loss of apoptotic control. The purpose of apoptosis is to kill abnormal cells and prevent tumor growth (34). The Bcl-2 family, consisting of the anti-apoptotic protein (Bcl-2) and pro-apoptotic proteins (Bax and Bcl-2 antagonist/killer 1), are coupled to the activation of caspase-3 and caspase-7 in regulating mitochondria-mediated apoptosis (35,36). Bax expression could also directly induce apoptosis, which has therapeutic relevance (37). Caspases, a family of cysteine proteases, are central regulators of apoptosis (16). Caspase-3 is an important key protease that is activated during cell apoptosis (38). The cleavage of PARP occurs by upstream caspase-3 molecules, which are key drivers of apoptosis in tumors (39). In the present study, overexpression of HSP20 downregulated the anti-apoptotic protein, Bcl-2, and upregulated pro-apoptotic Bax, cleaved PARP and cleaved caspase-3 levels, inducing BC cell apoptosis. Therefore, the

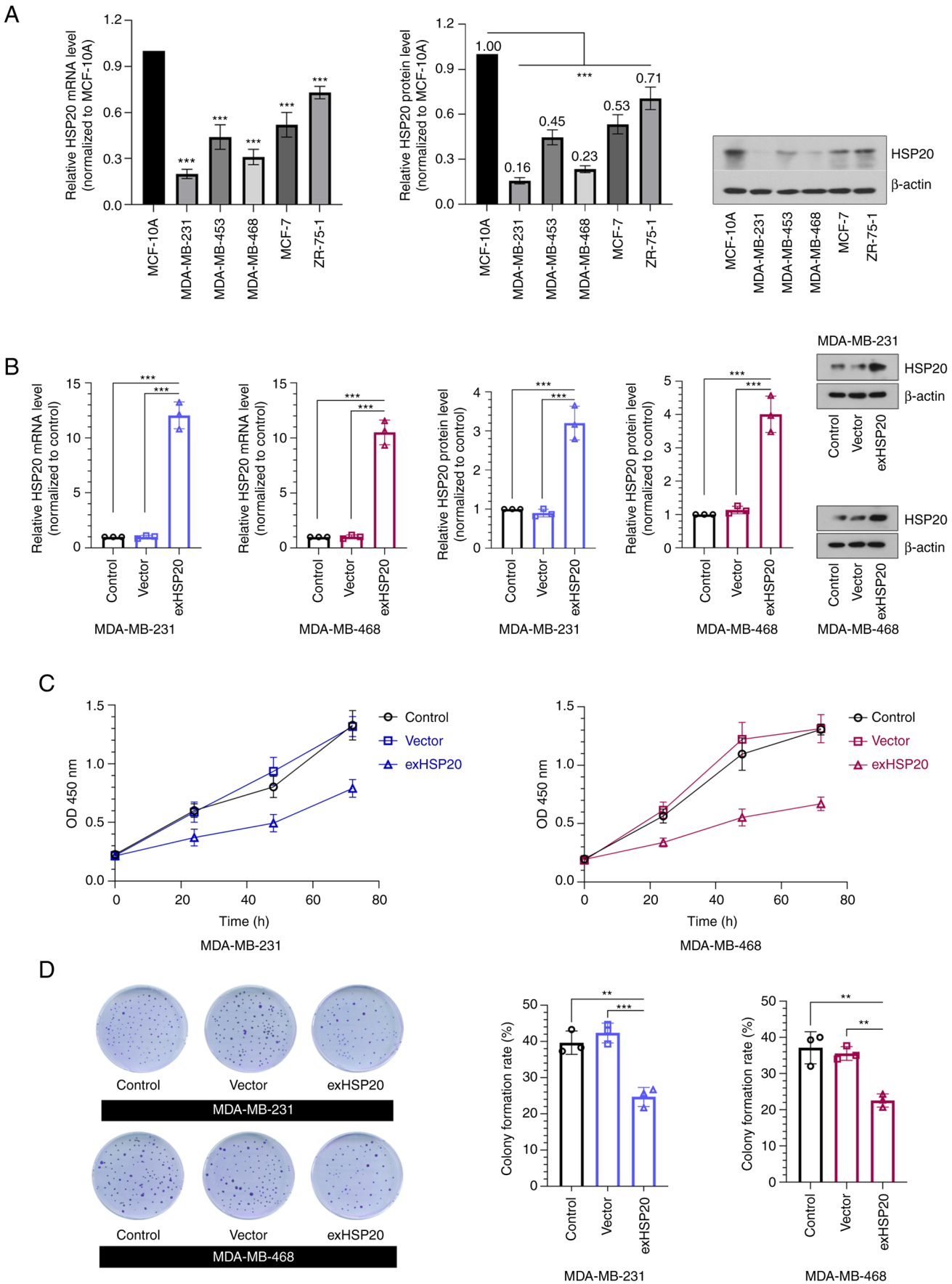

Figure 2. HSP20 overexpression inhibits BC cell proliferation. (A) Relative mRNA and protein expression levels of HSP20 in five BC cell lines compared with the MCF-10A normal mammary epithelial cell line. (B) Relative expression levels of HSP20 in MDA-MB-231 and MDA-MB-468 cells overexpressing HSP20. (C) Cell Counting Kit-8 proliferation assay. (D) Representative images and quantitative analysis of colony formation assays. Data are presented as the mean ± SD. **P<0.01; ***P<0.001 vs. MCF-10A or as indicated. BC, breast cancer; control, untransfected cells; vector, cells transfected with an empty vector; exHSP20, HSP20-overexpressing cells; HSP20, heat shock protein 20; OD, optical density.

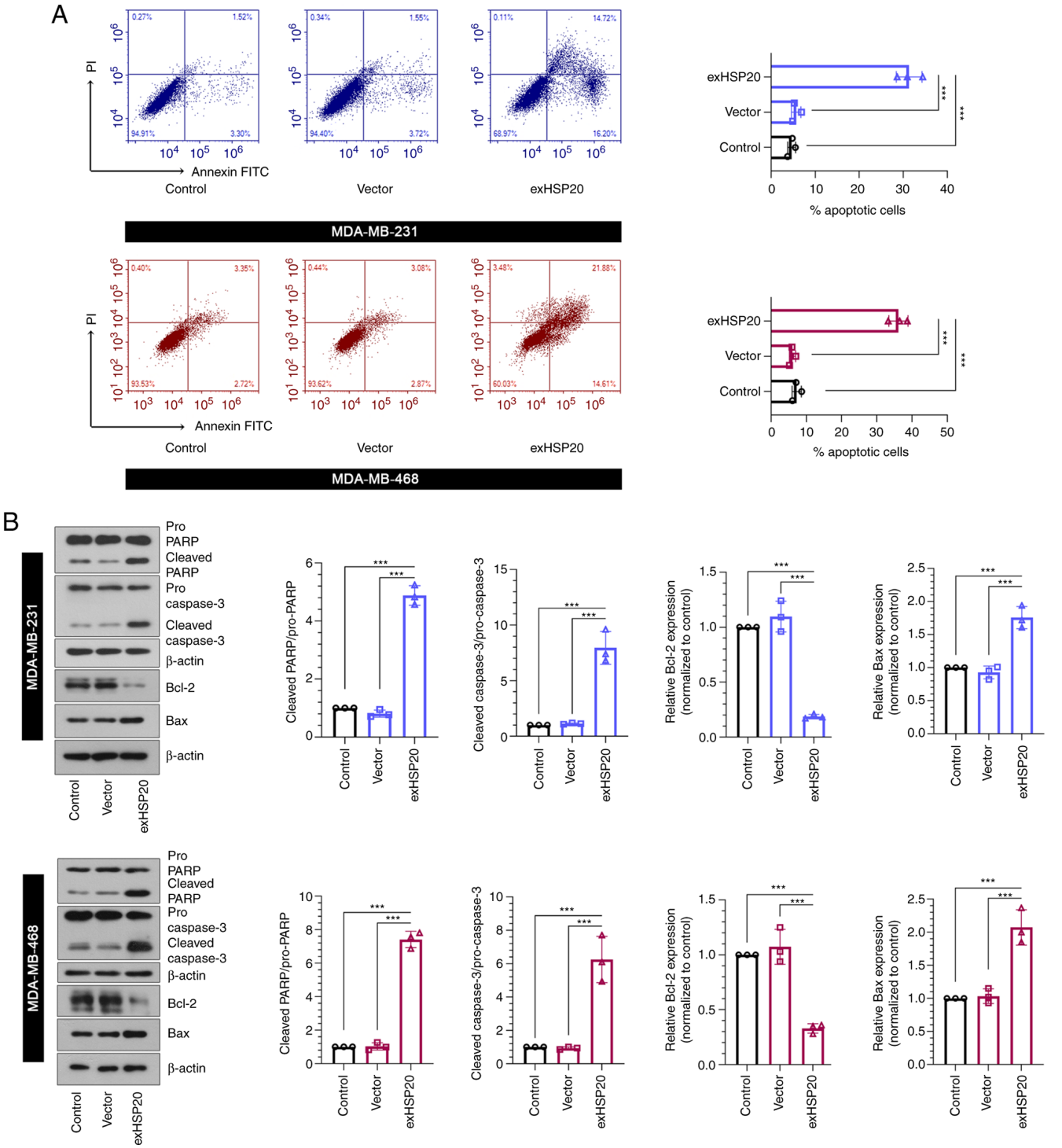

Figure 3. HSP20 overexpression contributes to breast cancer cell apoptosis. (A) Cellular apoptosis was examined via flow cytometry in transfected MDA-MB-231 and MDA-MB-468 cells. (B) Relative expression levels of apoptosis-related proteins in transfected MDA-MB-231 and MDA-MB-468 cells. Data are presented as the mean ± SD. ***P<0.001. HSP20, heat shock protein 20; control, untransfected cells; vector, cells transfected with an empty vector; exHSP20, HSP20-overexpressing cells; PARP, poly (ADP-ribose) polymerase.

overexpression of HSP20 in BC may induce the apoptosis of BC cells.

Cancer invasion and metastasis are multistep and complex processes, which have become a huge obstacle in the clinical treatment of various tumors (40,41). Furthermore, metastasis is one the major reasons for therapeutic failure in BC (42,43). Therefore, reducing cell migration and invasion effectively controls the metastasis of cancer cells. In the present study, it was found that the overexpression of HSP20 significantly inhibited the metastasis of BC cells, as identified using migration and invasion assays.

Additionally, the activation of the MAPK and AKT signaling pathways predicts a poor prognosis and the early recurrence of BC in patients (24). The MAPK signaling pathway is an important pathway in cell migration, and the inhibition of the MAPK signaling pathway can inhibit the

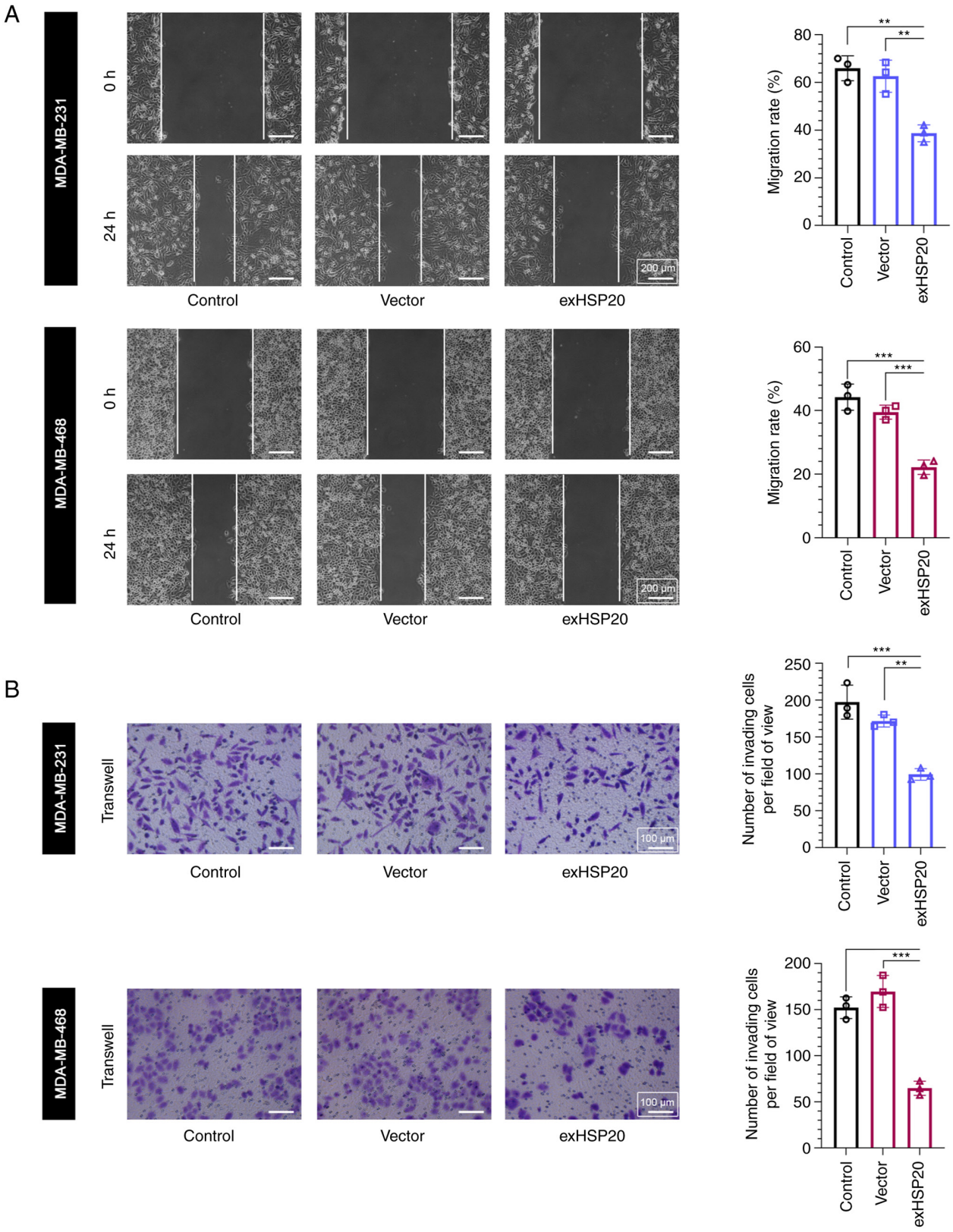

Figure 4. HSP20 overexpression suppresses breast cancer cell migration and invasion. (A) Wound healing assays were used to assess cell migration. HSP20 was overexpressed in MDA-MB-231 and MDA-MB-468 cells and images were captured at 0 and 24 h. Microscope magnification, x100. (B) Transwell assay of cell invasion in HSP20-overexpressing MDA-MB-231 and MDA-MB-468 cells. Microscope magnification, x200. Data are presented as the mean ± SD. **P<0.01; ***P<0.001. HSP20, heat shock protein 20; control, untransfected cells; vector, cells transfected with an empty vector; exHSP20, HSP20-overexpressing cells.

migration of BC cells (44). The MAPK pathway consists of ERK, JNK and p38; ERK is an important signal transducer for cell survival, and JNK and p38 contribute to acquiring invasion and migration capabilities (45). Accumulating evidence suggests that MAPK has the potential to prevent invasion and metastasis of various tumors (20,46).

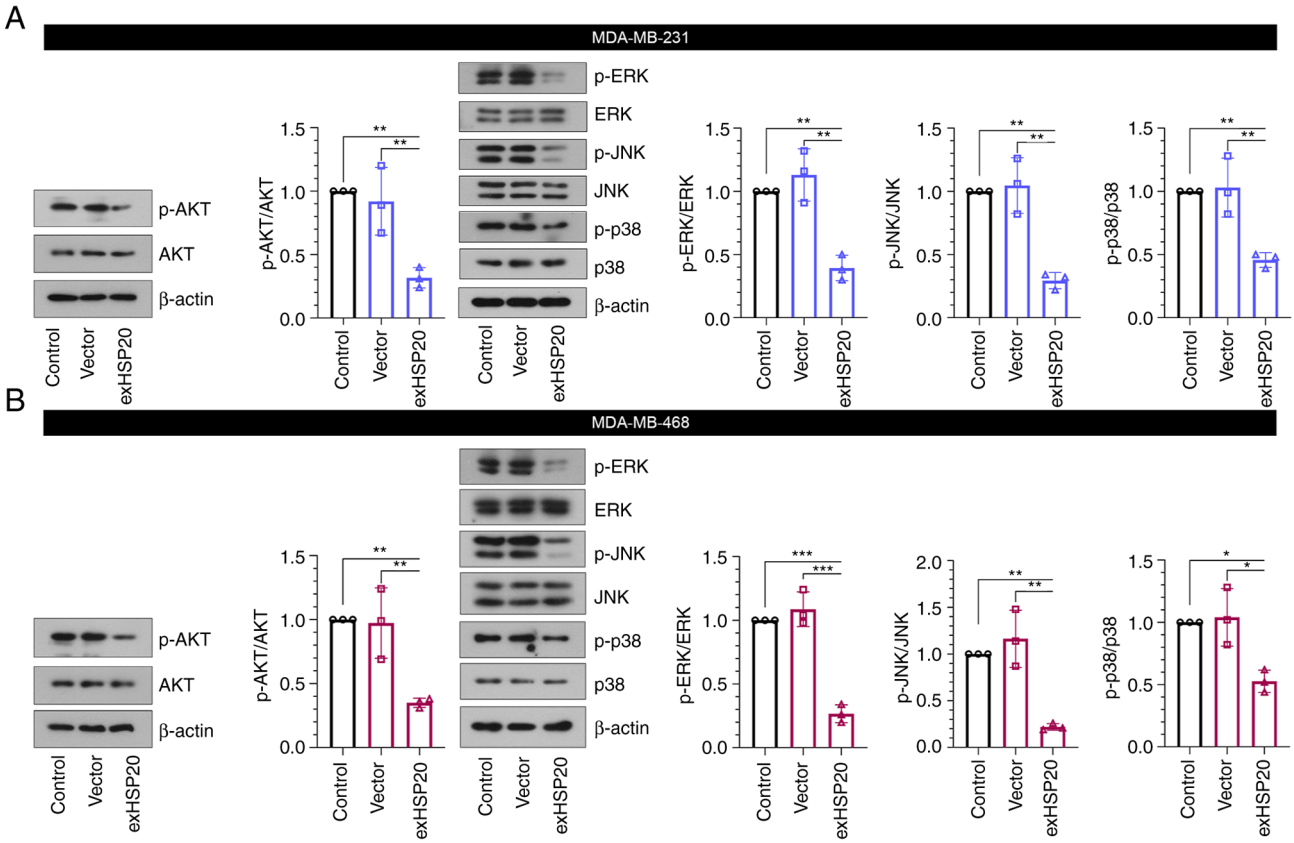

Figure 5. HSP20 overexpression inactivates the AKT and MAPK signaling pathways. Key proteins in the MAPK and AKT pathways were detected using western blot analysis in HSP20-overexpressing (A) MDA-MB-231 cells and (B) MDA-MB-468 cells. Data are presented as the mean ± SD. *P<0.05; **P<0.01; ***P<0.001. control, untransfected cells; vector, cells transfected with an empty vector; exHSP20, HSP20-overexpressing cells; HSP20, heat shock protein 20; p-, phosphorylated.

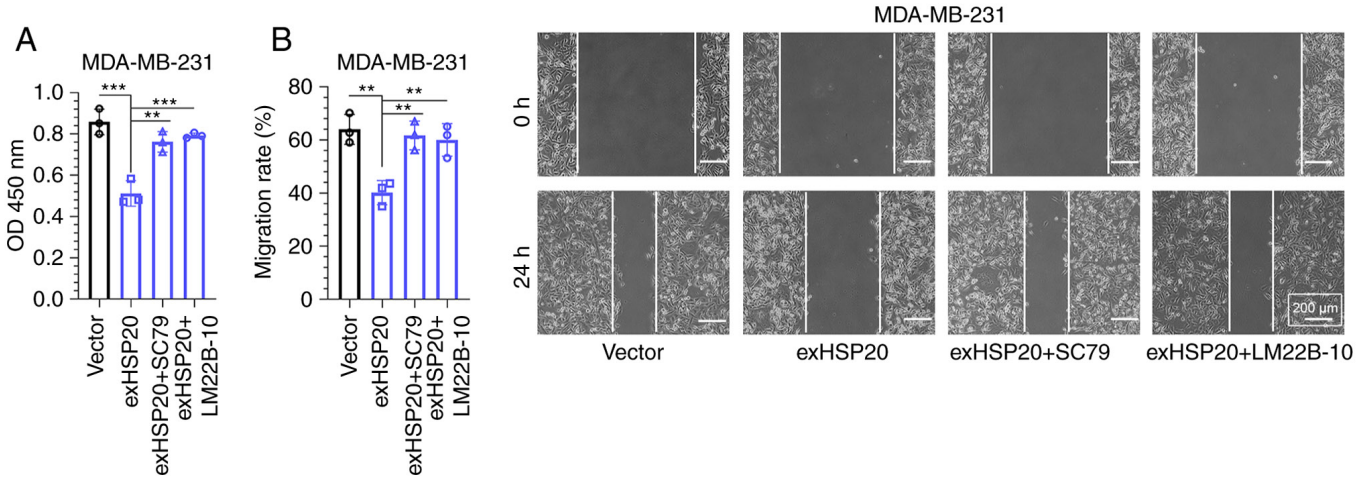

Figure 6. SC79 or LM22B-10 treatment reverses the inhibitory effects of HSP20 on cell proliferation and migration. (A) Cell Counting Kit-8 and (B) wound healing experiments were performed in HSP20-overexpressing MDA-MB-231 cells treated with 10 μM SC79 (an AKT agonist) or 50 μM LM22B-10 (an ERK agonist). Microscope magnification, x100. Data are presented as the mean ± SD. **P<0.01; ***P<0.001. vector, cells transfected with an empty vector; exHSP20, HSP20-overexpressing cells; HSP20, heat shock protein 20; OD, optical density.

Furthermore, the AKT signaling pathway participates in numerous cellular events, such as the cell cycle and glucose metabolism, particularly in cancer cells (47). In BC, the AKT signaling pathway is frequently activated, promoting BC cell invasion and metastasis (24,48). The present study demonstrated that overexpression of HSP20 inhibited MAPK and AKT signaling in BC.

In conclusion, the findings of the present study suggest that the downregulation of HSP20 in BC tissues may be associated with the progression of BC. In addition, HSP20

overexpression suppressed the malignant phenotype of BC cells. This effect may be associated with the inhibition of the AKT and MAPK signaling pathways. HSP20 may thus prove to be a potential prognostic marker or a candidate therapeutic target for BC.

Acknowledgements

Not applicable.

Funding

No funding was received.

Availability of data and materials

The datasets used and/or analyzed during the current study are available from the corresponding author on reasonable request.

Authors' contributions

YY, YW, LH, XG and GS performed the experiments. YY and HJ confirmed the authenticity of all the raw data. YY and YW wrote the manuscript. HJ designed this study and polished the manuscript. All authors read and approved the final manuscript.

Ethics approval and consent to participate

The present study was approved by the ethics committee of Wuxi 9th Affiliated Hospital of Soochow University (approval no. LW2021008; Wuxi, China), and written informed consent was provided by each participant.

Patient consent for publication

Not applicable.

Competing interests

The authors declare that they have no competing interests.

References

1. Ahmad A: Breast cancer statistics: Recent trends. Adv Exp Med Biol 1152: 1-7, 2019.
2. Singh SK, Singh S, Lillard JW Jr and Singh R: Drug delivery approaches for breast cancer. Int J Nanomedicine 12: 6205-6218, 2017.
3. Sultan AS, Marie MA and Sheweita SA: Novel mechanism of cannabidiol-induced apoptosis in breast cancer cell lines. Breast 41: 34-41, 2018.
4. Fan L, Strasser-Weippl K, Li JJ, St Louis J, Finkelstein DM, Yu KD, Chen WQ, Shao ZM and Goss PE: Breast cancer in China. Lancet Oncol 15: e279-e289, 2014.
5. McDonald ES, Clark AS, Tchou J, Zhang P and Freedman GM: Clinical diagnosis and management of breast cancer. J Nucl Med 57 (Suppl 1): 9S-16S, 2016.
6. Matsen CB and Neumayer LA: Breast cancer: A review for the general surgeon. JAMA Surg 148: 971-979, 2013.
7. He X, Wang J, Yu H, Lv W, Wang Y, Zhang Q, Liu Z and Wu Y: Clinical significance for diagnosis and prognosis of POP1 and its potential role in breast cancer: A comprehensive analysis based on multiple databases. Aging (Albany NY) 14: 6936-6956, 2022.
8. Dyan B, Seele PP, Skepu A, Mdluli PS, Mosebi S and Sibuyi NRS: A review of the nucleic acid-based lateral flow assay for detection of breast cancer from circulating biomarkers at a point-of-care in low income countries. Diagnostics (Basel) 12: 1973, 2022.
9. Sun YS, Zhao Z, Yang ZN, Xu F, Lu HJ, Zhu ZY, Shi W, Jiang J, Yao PP and Zhu HP: Risk factors and preventions of breast cancer. Int J Biol Sci 13: 1387-1397, 2017.
10. Liang Y, Zhang H, Song X and Yang Q: Metastatic heterogeneity of breast cancer: Molecular mechanism and potential therapeutic targets. Semin Cancer Biol 60: 14-27, 2020.
11. Li F, Xie Y, Wu Y, He M, Yang M, Fan Y, Li X, Qiao F and Deng D: HSP20 exerts a protective effect on preeclampsia by regulating function of trophoblast cells via Akt pathways. Reprod Sci 26: 961-971, 2019.
12. Fan GC, Chu G and Kranias EG: Hsp20 and its cardioprotection. Trends Cardiovasc Med 15: 138-141, 2005.
13. Noda T, Kumada T, Takai S, Matsushima-Nishiwaki R, Yoshimi N, Yasuda E, Kato K, Toyoda H, Kaneoka Y, Yamaguchi A and Kozawa O: Expression levels of heat shock protein 20 decrease in parallel with tumor progression in patients with hepatocellular carcinoma. Oncol Rep 17: 1309-1314, 2007.
14. Matsushima-Nishiwaki R, Adachi S, Yoshioka T, Yasuda E, Yamagishi Y, Matsuura J, Muko M, Iwamura R, Noda T, Toyoda H, *et al*: Suppression by heat shock protein 20 of hepatocellular carcinoma cell proliferation via inhibition of the mitogen-activated protein kinases and AKT pathways. J Cell Biochem 112: 3430-3439, 2011.
15. Nagasawa T, Matsushima-Nishiwaki R, Yasuda E, Matsuura J, Toyoda H, Kaneoka Y, Kumada T and Kozawa O: Heat shock protein 20 (HSPB6) regulates TNF-α-induced intracellular signaling pathway in human hepatocellular carcinoma cells. Arch Biochem Biophys 565: 1-8, 2015.
16. Nagasawa T, Matsushima-Nishiwaki R, Toyoda H, Matsuura J, Kumada T and Kozawa O: Heat shock protein 20 (HSPB6) regulates apoptosis in human hepatocellular carcinoma cells: Direct association with Bax. Oncol Rep 32: 1291-1295, 2014.
17. Ju YT, Kwag SJ, Park HJ, Jung EJ, Jeong CY, Jeong SH, Lee YJ, Choi SK, Kang KR, Hah YS and Hong SC: Decreased expression of heat shock protein 20 in colorectal cancer and its implication in tumorigenesis. J Cell Biochem 116: 277-286, 2015.
18. Pritchard AL and Hayward NK: Molecular pathways: Mitogen-activated protein kinase pathway mutations and drug resistance. Clin Cancer Res 19: 2301-2309, 2013.
19. Haddadi N, Lin Y, Travis G, Simpson AM, Nassif NT and McGowan EM: PTEN/PTENP1: 'Regulating the regulator of RTK-dependent PI3K/Akt signalling', new targets for cancer therapy. Mol Cancer 17: 37, 2018.
20. Reddy KB, Nabha SM and Atanaskova N: Role of MAP kinase in tumor progression and invasion. Cancer Metastasis Rev 22: 395-403, 2003.
21. Anjum J, Mitra S, Das R, Alam R, Mojumder A, Emran TB, Islam F, Rauf A, Hossain MJ, Aljohani ASM, *et al*: A renewed concept on the MAPK signaling pathway in cancers: Polyphenols as a choice of therapeutics. Pharmacol Res 184: 106398, 2022.
22. Asl ER, Amini M, Najafi S, Mansoori B, Mokhtarzadeh A, Mohammadi A, Lotfinejad P, Bagheri M, Shirjang S, Lotfi Z, *et al*: Interplay between MAPK/ERK signaling pathway and MicroRNAs: A crucial mechanism regulating cancer cell metabolism and tumor progression. Life Sci 278: 119499, 2021.
23. Huang S, Wang D, Zhang S, Huang X, Wang D, Ijaz M and Shi Y: Tunicamycin potentiates paclitaxel-induced apoptosis through inhibition of PI3K/AKT and MAPK pathways in breast cancer. Cancer Chemother Pharmacol 80: 685-696, 2017.
24. Chun J and Kim YS: Platycodin D inhibits migration, invasion, and growth of MDA-MB-231 human breast cancer cells via suppression of EGFR-mediated Akt and MAPK pathways. Chem Biol Interact 205: 212-221, 2013.
25. Zhao Y, Yang X, Xu X, Zhang J, Zhang L, Xu H, Miao Z, Li D and Wang S: Deubiquitinase PSMD7 regulates cell fate and is associated with disease progression in breast cancer. Am J Transl Res 12: 5433-5448, 2020.
26. Alam MS, Rahaman MM, Sultana A, Wang G and Mollah MNH: Statistics and network-based approaches to identify molecular mechanisms that drive the progression of breast cancer. Comput Biol Med 145: 105508, 2022.
27. Xuan Z, Zhang Y, Jiang J, Zheng X, Hu X, Yang X, Shao Y, Zhang G and Huang P: Integrative genomic analysis of N6-methyladenosine-single nucleotide polymorphisms (m^6A-SNPs) associated with breast cancer. Bioengineered 12: 2389-2397, 2021.

28. Livak KJ and Schmittgen TD: Analysis of relative gene expression data using real-time quantitative PCR and the 2(-Delta Delta C(T)) method. Methods 25: 402-408, 2001.
29. Cserni G, Chmielik E, Cserni B and Tot T: The new TNM-based staging of breast cancer. Virchows Arch 472: 697-703, 2018.
30. Brook N, Brook E, Dharmarajan A, Dass CR and Chan A: Breast cancer bone metastases: Pathogenesis and therapeutic targets. Int J Biochem Cell Biol 96: 63-78, 2018.
31. Winters S, Martin C, Murphy D and Shokar NK: Breast cancer epidemiology, prevention, and screening. Prog Mol Biol Transl Sci 151: 1-32, 2017.
32. Li R, Shi Y, Zhao S, Shi T and Zhang G: NF-κB signaling and integrin-β1 inhibition attenuates osteosarcoma metastasis via increased cell apoptosis. Int J Biol Macromol 123: 1035-1043, 2019.
33. Martin TP, Currie S and Baillie GS: The cardioprotective role of small heat-shock protein 20. Biochem Soc Trans 42: 270-273, 2014.
34. Tunjung WAS and Sayekti PR: Apoptosis induction on human breast cancer T47D cell line by extracts of Ancorina sp. F1000Res 8: 168, 2019.
35. Li XX, Wang DQ, Sui CG, Meng FD, Sun SL, Zheng J and Jiang YH: Oleandrin induces apoptosis via activating endoplasmic reticulum stress in breast cancer cells. Biomed Pharmacother 124: 109852, 2020.
36. Pluta P, Smolewski P, Pluta A, Cebula-Obrzut B, Wierzbowska A, Nejc D, Robak T, Kordek R, Gottwald L, Piekarski J and Jeziorski A: Significance of Bax expression in breast cancer patients. Pol Przegl Chir 83: 549-553, 2011.
37. Bumbat M, Wang M, Liang W, Ye P, Sun W and Liu B: Effects of Me_2SO and trehalose on the cell viability, proliferation, and Bcl-2 family gene (BCL-2, BAX, and BAD) expression in cryopreserved human breast cancer cells. Biopreserv Biobank 18: 33-40, 2020.
38. Affar EB, Germain M, Winstall E, Vodenicharov M, Shah RG, Salvesen GS and Poirier GG: Caspase-3-mediated processing of poly(ADP-ribose) glycohydrolase during apoptosis. J Biol Chem 276: 2935-2942, 2001.
39. Noble P, Vyas M, Al-Attar A, Durrant S, Scholefield J and Durrant L: High levels of cleaved caspase-3 in colorectal tumour stroma predict good survival. Br J Cancer 108: 2097-2105, 2013.
40. Uekita T and Sakai R: Roles of CUB domain-containing protein 1 signaling in cancer invasion and metastasis. Cancer Sci 102: 1943-1948, 2011.
41. Friedl P, Locker J, Sahai E and Segall JE: Classifying collective cancer cell invasion. Nat Cell Biol 14: 777-783, 2012.
42. Dattachoudhury S, Sharma R, Kumar A and Jaganathan BG: Sorafenib inhibits proliferation, migration and invasion of breast cancer cells. Oncology 98: 478-486, 2020.
43. Sun B, Zhang S, Zhang D, Li Y, Zhao X, Luo Y and Guo Y: Identification of metastasis-related proteins and their clinical relevance to triple-negative human breast cancer. Clin Cancer Res 14: 7050-7059, 2008.
44. Matsushima-Nishiwaki R, Toyoda H, Nagasawa T, Yasuda E, Chiba N, Okuda S, Maeda A, Kaneoka Y, Kumada T and Kozawa O: Phosphorylated heat shock protein 20 (HSPB6) regulates transforming growth factor-α-induced migration and invasion of hepatocellular carcinoma cells. PLoS One 11: e0151907, 2016.
45. Igaki T, Pagliarini RA and Xu T: Loss of cell polarity drives tumor growth and invasion through JNK activation in Drosophila. Curr Biol 16: 1139-1146, 2006.
46. Chen PN, Hsieh YS, Chiang CL, Chiou HL, Yang SF and Chu SC: Silibinin inhibits invasion of oral cancer cells by suppressing the MAPK pathway. J Dent Res 85: 220-225, 2006.
47. Matsushima-Nishiwaki R, Toyoda H, Takamatsu R, Yasuda E, Okuda S, Maeda A, Kaneoka Y, Yoshimi N, Kumada T and Kozawa O: Heat shock protein 22 (HSPB8) reduces the migration of hepatocellular carcinoma cells through the suppression of the phosphoinositide 3-kinase (PI3K)/AKT pathway. Biochim Biophys Acta Mol Basis Dis 1863: 1629-1639, 2017.
48. Kulawiec M, Owens KM and Singh KK: Cancer cell mitochondria confer apoptosis resistance and promote metastasis. Cancer Biol Ther 8: 1378-1385, 2009.